Article

Impact of Conservation Agriculture on Soil Erosion in the Annual Cropland of the Apulia Region (Southern Italy) Based on the RUSLE-GIS-GEE Framework

Matteo Petito [1], Silvia Cantalamessa [2], Giancarlo Pagnani [2], Francesco Degiorgio [3], Barbara Parisse [4] and Michele Pisante [2,*]

[1] Department of Agronomy, Food, Natural Resources, Animals and Environment, University of Padova, Viale dell'Università 16, 35020 Legnaro, Italy; matteo.petito@phd.unipd.it

[2] Faculty of Bioscience and Technologies for Food, Agriculture and Environment, University of Teramo, Via Balzarini, 1, 64100 Teramo, Italy; scantalamessa@unite.it (S.C.); gpagnani@unite.it (G.P.)

[3] Regione Puglia, Direzione Dipartimento Agricoltura, Sviluppo Rurale e Ambiente, Lungomare Nazario Sauro, 4, 70121 Bari, Italy; f.degiorgio@regione.puglia.it

[4] Council for Agricultural Research and Economics (CREA), Agriculture and Environment, Via della Navicella 4, 00185 Roma, Italy; barbara.parisse@crea.gov.it

* Correspondence: mpisante@unite.it

Abstract: The processes of soil erosion and land degradation are more rapid in the case of inappropriate agricultural management, which leads to increased soil loss rates. Moreover, climatic conditions are one of the most important determining factors affecting agriculture, especially in the Mediterranean areas featuring irregular rainfall and high summer temperatures. Conservation agriculture (CA) can make a significant contribution to reducing soil erosion risk on the annual cropland (ACL) of the Mediterranean region in comparison with conventional management (CM). The objective of this study is to provide soil loss rate maps and calculate the values for each altitude and slope class and their combination for the Apulia region in four annual production cycles for the scenarios CM and CA. The present study estimates the significance of the adoption of CA on soil erosion assessment at regional scale based on the Revised Universal Soil Loss Equation (RUSLE) model. The parameters of the RUSLE model were estimated by using remote sensing (RS) data. The erosion probability zones were determined through a Geographic Information System (GIS) and Google Earth Engine (GEE) approach. Digital terrain model (DTM) at 8 m, ACL maps of the Apulia region, and rainfall and soil data were used as an input to identify the most erosion-prone areas. Our results show a 7.5% average decrease of soil loss rate during the first period of adoption of the four-year crop cycle—from 2.3 t ha^{-1} y^{-1} with CM to 2.1 t ha^{-1} y^{-1} with the CA system. CA reduced soil loss rate compared to CM in all classes, from 10.1% in hill class to 14.1% for hill + low slope class. These results can therefore assist in the implementation of effective soil management systems and conservation practices to reduce soil erosion risk in the Apulia region and in the Mediterranean basin more generally.

Keywords: agriculture management system; altitude; Mediterranean; remote sensing; slope; soil loss rate

1. Introduction

Soil erosion is one of the main parameters for assessing soil quality [1–3]. It is defined as "the movement and transport of soil by various agents, particularly water, wind, and mass movement" [4]. In addition, soil quality is defined "the capacity of a soil to function, within natural or managed ecosystem boundaries, to sustain plant and animal productivity, to maintain or enhance water and air quality, and support human health

and habitation" [5]. Soil erosion and soil quality are strongly correlated phenomena. Soil quality affects the rate of soil loss and is in turn affected by it. Erosion effects on soil quality are determined by land use, farming system and management, spatial variability in erosional processes, and inherent soil properties [6]. Erosion affects soil quality and productivity, reducing infiltration rates, organic matter, nutrients, water-holding capacity, soil biota, and depth with considerable impacts on soil environment [7,8]. Soil erosion also has a negative impact on ecosystem services such as water quality and quantity, biodiversity, and crop yields [9,10].

Land degradation by water mainly affects Southern Italian regions, where fragile soils are exposed to long periods of drought followed by heavy bursts of erosive rainfall falling on steep slopes, resulting in considerable amounts of soil loss rate [11,12].

Soil erosion by water refers to the depletion of the ground surface by water and gravity which results in dislodgment of soil particles and their entrainment, transport, and deposition [13]. It occurs when either rain splashes or water flows over the surface, thus causing the particles of soil to detach and drift [14]. Climate change and intensive agricultural practices are current drivers increasing soil erosion risk and reducing soil functions [15,16], which result in a general degradation of soil quality [17–19]. Regions already affected by climate change are the drought-affected areas of the EU, especially in the Mediterranean, such as in Spain, Greece, and Southern Italy, where climate change has already had visible impacts on yields and soils [20]. In addition, European soils suffer from high degradation rates because of the use of intensive agricultural practices that are unsustainable in the long term [21]. Moreover, land-use management decisions have a direct impact on the soil loss rate, especially in arable land [22]. In 2006, the European Commission (EC) classified soil erosion as the first among eight major threats to soil in its topic-specific Soil Thematic Strategy [23].

Agricultural land-use practices including erosion-prone ground cover or crops providing inadequate ground cover significantly accelerate soil erosion phenomena [24,25]. Among these practices is included CM, which is based on mechanical tillage, monoculture, or, alternatively, a crop sequence, crop residues burned, buried, or removed [26,27]. In this context, the adoption of sustainable agricultural systems such as CA represents an effective and viable option for reducing erosion and land degradation. CA is an agricultural practice based on three interlinked principles: (i) continuous no or minimum mechanical soil disturbance; (ii) permanent maintenance of soil mulch cover; and (iii) diversification of cropping system. The adoption of CA has proved to be beneficial to the soil and to reduce erosion, while also increasing organic matter and fertility, as well as water infiltration and retention, thus reducing runoffs, improving water quality, and increasing water holding capacity [28–30]. Usually, significant measurable benefits of CA in annual cropland and the rehabilitation of soil-related ecosystem functions and services may take a longer time to take effect—roughly three to seven years [31].

Acknowledgement of threats such as erosion, compaction, and salinization led to the implementation of new sustainability objectives in the renewed Common Agricultural Policy (CAP) 2014–2020 in the European Union (EU) and in accordance with the new EU soil strategy for 2030 (https://ec.europa.eu/environment/publications/eu-soil-strategy-2030_en, accessed on 13 January 2022) and also the Farm to Fork strategy (https://ec.europa.eu/food/horizontal-topics/farm-fork-strategy_en, accessed on 13 January 2022). Policies supporting CA can be found in the so-called second pillar of the CAP, which aims to contribute "to the development of an agricultural sector of the Union characterized by a greater territorial and environmental balance and more respectful of the climate, resilient, competitive and innovative" and also to the "development of rural territories" (EU Reg. 1305/2013). CA regulations are defined within European policy guidelines that can be found within the Rural Development Program (RDP) under the sub-measure 10.1 (M10.1), whose adoption is compulsory. This measure "aims to preserve and promote the necessary changes to agricultural practices that make a positive

contribution to the environment and climate" (EU Reg. 1305/2013). Taking stock of these considerations, the present contribution is concerned with monitoring and evaluating how the adoption of CA contributes to reduce or stop soil erosion risk caused by water. Several modeling approaches have been conducted so far to assess soil erosion, for example, the Pan-European Soil Erosion Risk Assessment (PESERA) model and erosion rates based on runoff plot data [32,33]. However, as pointed out by Panagos et al. [32], such models do not capture the effects of conservation practices and their potential to mitigate soil erosion risk. Thus, even the effectiveness of policies that promote such practices cannot be addressed adequately. On the other hand, this becomes possible by adopting other models, such as the RUSLE, which has been used in the past years to monitor erosion, and which is specific to the EU context [34]. Moreover, soil erosion is one of the agro-environmental indicators adopted by the European Commission services for monitoring agricultural and environmental policies. This model can capture the impact of land-use changes, and thus highlight the efficacy that the European agri-environmental policies would have on restoring soil health [32,34]. Such a model has been used to estimate soil loss rate in several Mediterranean areas [35].

The objective of this study is to provide soil loss rate maps and calculate the averaged values for each altitude and slope class and their combination for the ACL of Apulia region for both the scenarios. This part of Italy suffers from heavy rainfall (fall/winter period) as well as decreasing precipitation. Moreover, increase of temperatures and consequently drier conditions (summer) caused by more and more evident effects of climate change and CM pose an additional threat to Apulian cropland [36,37]. Our approach is based on the RUSLE-GIS-GEE framework [3,38], using more suited databases at regional scale. This could provide greater detail and accuracy in calculating soil loss rate for ACL, separately for the two management systems: CM and CA for the period 2016–2020, following the introduction in 2016 of the specific sub-measure M10.1 "Conservation Agriculture", in which only a part of the farmers participated, being a voluntary measure.

2. Materials and Methods

2.1. Study Area

The Apulia region (Figure 1) is situated in the southeastern part of the boot-shaped Italian Peninsula bordering the Adriatic and Ionian seas along the east and southeast coasts, respectively. The region is divided into 257 municipalities grouped into five provinces and covers a surface area of approximately 19,500 km². The region is characterized by low mountains located in the Gargano promontory and in the Daunian Sub-Apennine, respectively, in the north and east of the Foggia province; the Tavoliere plain (the second largest plain in Italy), which extends for 3000 km² in the central and southern part of the Foggia province; and the Murgia plateau, which covers a surface of 4000 km² between the provinces of Barletta–Andria–Trani and Bari [39]. The Apulia region features hot and dry summer seasons, as well as mild and rainy winter seasons typical of semiarid Mediterranean climate. Annual precipitation varies between 450 and 550 mm in much of the region (two-thirds concentrated from autumn to winter). The highest values of precipitation, with more than 900 mm y⁻¹, are observed in the Gargano area, in the province of Foggia, whereas the lowest values, around 400 mm y⁻¹, are observed in the Tavoliere plain. The hydrological regimes are irregular, of torrential type, with high stream and river flow rates during the rainy season and practically no water flow in summer [37]. Agriculture plays a very important role in the economic context of the Italian territory; this region is second in terms of production of olive oil, wine, and fresh vegetables. Particularly important is the production of durum wheat in the Tavoliere plain, orchards (cherries and figs) near Bari, and tobacco in the province of Lecce [40]. Durum wheat and, in general, cereals (barley, rye, oats) are the most important typical ACL in Apulia region. For ACL in Southern Italy, the period between 15 October to 1 August corresponds approximately to the period from sowing to harvesting.
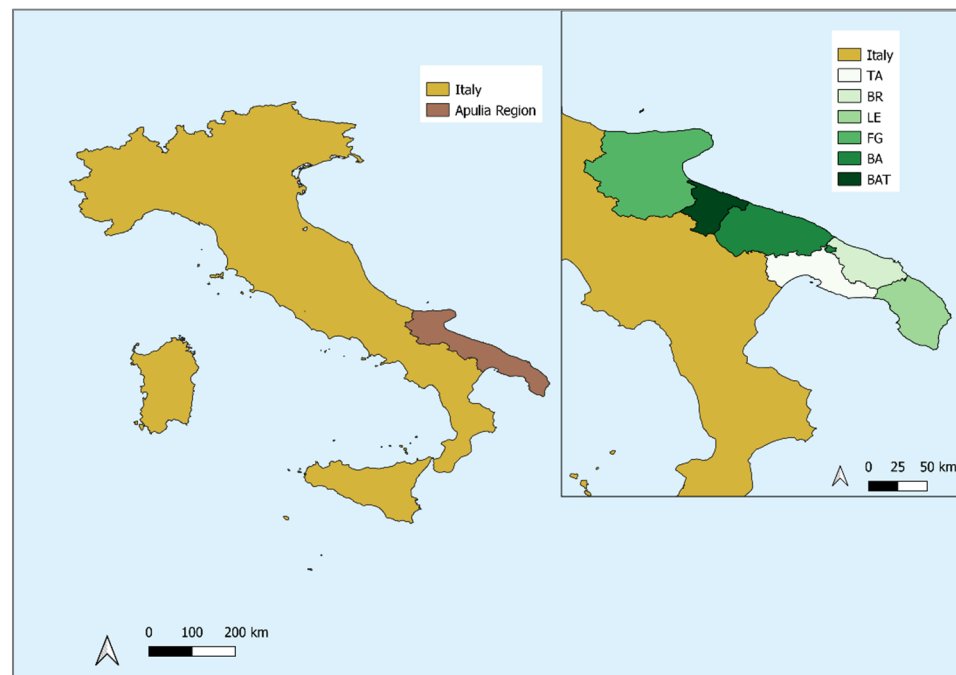
Figure 1. Study area. Apulia region according to NUTS 2021 classification. Provinces of Apulia region are Taranto (TA), Brindisi (BR), Lecce (LE), Foggia (FG), Bari (BA), and Barletta–Andria–Trani (BAT).

2.2. Soil Loss Modeling: RUSLE Factors

The RUSLE model has been widely used for both agricultural and natural land to estimate annual soil loss rate and to evaluate soil erosion risk [41,42]. This model is accurate, easy to apply, and needs a moderate amount of data. Its usage has increased over the past few decades, particularly with the increase of RS and GIS applications [43,44]. The advent of RS and GIS application has increased the interest in developing new methods of calculation and sharing data, using cloud-computing platforms. GEE was developed as an open-source platform for analyzing geospatial data. GEE has been used worldwide for retrieving and processing many Earth observation data, which nowadays cover all geospatial data needed to build the RUSLE-GIS-GEE framework in a comprehensive and robust cloud-based environment. GEE's capabilities can be used to process large amounts of geospatial data: especially, with improvements in these data's availability and processing time, for this reason, it is successfully used in several fields on both regional and global scales [45–47]. In the current study, soil loss rate estimation based on RUSLE was implemented in the GEE environment to increase the ability to determine susceptibility to erosion risk.

The RUSLE model [48,49] was used to estimate the soil loss rate for the scenarios for the CM and CA system in the Apulia region with limited annual cropland for the first period of adoption (2016–2020). RUSLE provides an ideal framework to assess soil loss rate and its factors for both the scenarios. Specifically, RUSLE considers support practices (*P*), rainfall (*R*), soil erodibility (*K*), topography (*LS*), and cover management (*C*) as important factors affecting soil loss rate. RUSLE can be mathematically expressed as

$$A = R \times K \times LS \times C \times P \tag{1}$$

where *A* (Mg ha^{-1} y^{-1}) is the longtime average annual soil loss rate, *R* (MJ mm h^{-1} ha^{-1} y^{-1}) is the rainfall erosivity factor, *K* (Mg h MJ^{-1} mm^{-1}) is the soil erodibility factor, *LS* (unitless) is the slope length factor and slope steepness factor, *C* (unitless) is the land cover and management factor, and *P* (unitless) is the soil conservation or prevention practices factor [49].

2.2.1. R-Factor

R-factor is an index of rainfall erosivity that quantifies the potential capacity of rain to cause erosion [49]. The factors that are affected by rainfall erosivity are amount, intensity, terminal velocity, drop size, and drop size distribution of rain [50]. For a given location, it is the long-term average of the annual R_{aj} values which, in turn, are given by the sum of all the erosion index (*EI*) single-storm EI_{30} values for year j [51].

The annual rainfall-runoff erosivity (*R*-factor) values (MJ mm h^{-1} ha^{-1} y^{-1}) for Italy were computed by the following equation [51]:

$$R = \frac{1}{N}\sum_{1}^{N} EI_{30-annual} \tag{2}$$

where *N* is an *N*-year period, and *EI* is the rainfall erosivity index (MJ mm ha^{-1} h^{-1}), expressed as

$$EI_{30-annual} = 12.142(abc)^{0.6446} \tag{3}$$

Where the variables *a*, *b*, and *c* are the annual precipitation, the maximum annual daily precipitation, and the maximum annual hourly precipitation, respectively—all expressed in centimeters. Variable *a* represents less erosive precipitations, with a cumulative effect over a long period. Variables *b* and *c* describe very erosive effects due to extreme rainfalls in storms and heavy showers.

This study estimated the *R*-factor based on ERA5-Land (E5L) gridded weather data, freely available as product of the Copernicus Climate Change Service (C3S). The E5L is a high-resolution reanalysis dataset which covers the period from 1981 to present on a regular grid with a spatial resolution of 0.1° × 0.1° latitude–longitude referred to as geographic coordinate system WGS84 (EPSG:4326), corresponding to a horizontal resolution of 9 km. The data are provided with an hourly time-step and released with a delay of 2–3 months from present.

All grid cells (for a total of 231) located in the Apulia region were considered for retrieving total hourly precipitation (estimated in millimeters, mm) for the period from January 1981 to December 2019. The accumulated precipitation values were processed to derive the total hourly precipitation (mm) from 00 UTC to the hour ending at the forecast step.

The *R*-factor was calculated as average of *EI* yearly values regarding four N-year periods: 1981–2016, 1981–2017, 1981–2018, and 1981–2019. *R*-factor descriptive statistics, such as minimum, maximum, standard deviation, and weighted average values, for the Apulia region were estimated, and the results are listed in Table S1. Data processing was performed through R (R Core Team, 2020). For RUSLE calculation (see Section 2.4), the results obtained for *R*-factor were projected into the EPSG: 3035 reference system and then masked for the ACL 2015 (1981–2016) and for ACL 2018 (1981–2017, 1981–2018, and 1981–2019) in GEE (Table S1).

2.2.2. K-Factor

The *K*-factor is the soil erodibility factor (t ha h ha^{-1} MJ^{-1} mm^{-1}), an empirical parameter based on the measurements of specific soil erodibility [52]. This parameter is measured based on these soil properties: texture, organic matter, structure, and permeability of the topsoil profile [53]. In this study, the reference value of *K*-factor is the one obtained from the "Soil Erodibility in Europe High Resolution dataset" [53] provided by the Joint Research Center (JRC) of European Soil Data Centre (ESDAC) and clipped for the Apulia region by using QGIS. The *K*-factor is estimated for the 20,000 field sampling points (133 for Apulia region) included in the Land Use/Cover Area frame (Land Use and Coverage Area, LUCAS) survey [54] and then interpolated with a Cubist regression model [55] using spatial covariates such as remotely sensed data and terrain features to produce a 500 m resolution *K*-factor map of Europe [53].

2.2.3. P-Factor

Support practice (*P*-factor) is an expression of the effects of agricultural management practices that reduce the erosion potential of runoff by influencing drainage patterns and the concentration and velocity of runoff [52]. The adoption of supporting conservation practices decreases the p value, which ranges between 0.2 (terraces with reverse slope) and 1.0 (no erosion control practices). The average value is estimated at around 0.95 in agricultural land, and for the EU it is estimated at 0.97. This effect is considerably greater in sensitive regions such as the Mediterranean area, although the reduction rate can generally be relatively small when adopting supportive practices [56]. In the present study, the reference value of *P*-factor is the one obtained from the EU datasets [57] provided by the JRC's ESDAC with 1 km resolution, and then clipped for the Apulia region by using QGIS.

2.2.4. LS-Factor

In the RUSLE model, the *L* and *S* factors represent the influence of the terrain topography on the sediment transport capacity of the overland flow [52]. Slope length (*L*) is defined as the point where overland flow starts to the point in which deposition occurs or runoff waters are channelized [58]. Slope steepness (*S*) describes how erosion increases with slope angle [58]. The combined *LS*-factor (dimensionless) describes the potential of surface runoff in accelerating soil loss rate, and, in most studies, determines the spatial resolution (cell size) of the modeled soil loss estimates. The topographic *LS*-factor was calculated by using the 8 m high-resolution DTM provided by the Apulia region (available on http://www.sit.puglia.it, accessed on 13 January 2022).

The *LS*-calculation was performed by using the equation proposed by Desmet and Govers [59]:

$$L_{i,j} = \frac{(A_{i,j} + D^2)^{m+1} - A_{i,j-in}^{m+1}}{D^{m+2} * x_{i,j}^{m} * 22.13^m} \tag{4}$$

where $A_{i,j-in}$ is the contributing area at the inlet of grid cell (*i,j*), measured in m². *D* is the grid cell size (meters), $X_{i,j} = sin\alpha_{i,j} + cos\alpha_{i,j}$, the $\alpha_{i,j}$ is the aspect direction of the grid cell (*i,j*). This equation was implemented by using the System for Automated Geoscientific Analyses (SAGA) software in QGIS, which incorporates a multiple flow algorithm and contributes to a precise estimation of flow accumulation [58]. It provides a comprehensive set of modules for data analysis, focusing on DTMs and terrain analysis [60,61]. A multiple flow algorithm present in SAGA (*LS*-factor field based) allows the calculation of *LS*-factor [58].

2.2.5. C-Factor

Among the inputs of RUSLE, the cover and management factor (*C*-factor) is the one most sensitive factor [62] that ranges between 0 and 1. The *C*-factor follows plant growth and rainfall dynamics [52,63] and can be managed by farmers and managers to control soil erosion in agricultural activities [34]. The *C*-factor represents the effect of cropping and management practices on soil erosion by water [49]. The decrease of the *C*-factor can be promoted by changing the amount of vegetation cover and tillage practices and soil management measures (e.g., reduced or no tillage and cover crop residues) that protect the soil surface, disperse raindrop energy, and reduce surface runoff [34,49]. Land-use types, crop rotation, and cultivation and management practices show obvious spatial and temporal variations that affect the accuracy of the *C*-factor estimate, ultimately affecting soil loss rate estimated by RUSLE [64,65]. Therefore, it is necessary to improve the ability to capture the space–time dynamics of the *C*-factor. In our study, to estimate the *C*-factor within the ACL of the Apulia region, we started from the equation proposed by Panagos et al. [34]:

$$C_{arable} = C_{crop} \times C_{managment} \qquad (5)$$

where C_{crop} is the *C*-factor based on the crop composition of an agricultural area, and $C_{management}$ quantifies the influence of management practices (reduced tillage, cover crop, and crop residues) on soil loss rate reduction. With regard to $C_{management}$, the combined effect of tillage practice ($C_{tillage}$), plant residues ($C_{residues}$), and cover crops (C_{cover}) was taken into account for the estimation of management factor [34]:

$$C_{managment} = C_{tillage} \times C_{residues} \times C_{cover} \qquad (6)$$

where a value of 0.176 was used for CA. This value was derived from the multiplication of the three factors adopted for CA ($C_{tillage}$ = 0.25; $C_{residues}$ = 0.88; C_{cover} = 0.80) [34], while a value of 1 was used for CM, in accordance with the multiplication of three factors adopted for CM ($C_{tillage}$ = 1; $C_{residues}$ = 1; C_{cover} = 1) [34].

Instead, C_{crop} was estimated by taking into account the Normalized Difference Vegetation Index (NDVI), as proposed by van der Knijff et al. [12], for regional-scale applications:

$$C_{crop} = \exp\left[-\alpha \frac{NDVI}{(\beta - NDVI)}\right] \qquad (7)$$

where α and β are parameters of the NDVI-C correlation. An α-value of 2 and a β-value of 1 seem to give reasonable results, because these values permit achieving a linear relationship, according to van der Knijff et al. [66]. This method has been employed by several studies worldwide [67–70]. In the present work, the *C*-factor was calculated for Apulia ACL as follows:

$$C = \exp\left[-\alpha \frac{NDVI}{(\beta - NDVI)}\right] X \, C_{management} \qquad (8)$$

For the calculation of *C*-factor's NDVI, GEE provides Sentinel-2 images that have a resolution of 10 m and are available for the two layers: bottom of atmosphere (BOA), level 2A) and top of atmosphere (TOA), level 1C). The TOA level is not provided with atmospheric correction, while the BOA level has atmospheric correction due to Sen2Cor [71]. The noncorrect atmospheric images have been continuously available since the launch of the satellite (23 May 2015), while the corrected ones have been available since 28 March 2017. As shown in the literature [72,73], there is a correlation between vegetational indices calculated at the two different layers (NDVI BOA > NDVI TOA). Subsequently, the correction factor between NDVI is calculated at the two levels, without which the *C*-factor would have been underestimated. We proceeded by calculating the NDVI Sentinel-2 at level 2a over the whole region for the interval from 1 April 2017 to 28 January 2021, by taking into consideration 2033 images in which NDVI was calculated both at the BOA and TOA level. The correction factor shows an average increase between TOA and BOA of 27% in the whole Apulia region and an increase of 29% in ACL. For the period 2016–2017, NDVI is calculated by using NDVI level 1c added to correction factor. The annual interval for each NDVI calculation is considered for the period between 15 October to 1 August of the following year, as it corresponds approximately to the period from sowing to harvesting in Southern Italy. Table 1 reports the number of images that have a cloudy pixel percentage lower than 20% and are processed for the calculation of each NDVI. Finally, the calculation of the two factors, *C* crop [38,74] and *C* management, and their multiplication, is possible in GEE environment.

Table 1. *C*-factor and NDVI values of ACL of the four cycles and two management systems.

Agricultural Seasons	Images (n)	Mean of NDVI (15/10–01/08)	C_{factor} CM	C_{factor} CA	%
2016–2017	309	0.3653	0.3268	0.3122	−4.5
2017–2018	415	0.3995	0.2742	0.2623	−4.3
2018–2019	408	0.3985	0.2803	0.2684	−4.2

| 2019–2020 | 449 | 0.4078 | 0.2656 | 0.2552 | −3.9 |
| Mean | | 0.3928 | 0.2867 | 0.2745 | −4.2 |

CM = conventional management. CA = conservation agriculture. NDVI = Normalized Difference Vegetation Index.

2.3. Identification of ACL

ACL areas are calculated using LUCAS points, which is a network that gives accurate and detailed information, it aims at computing statistical estimates at EU level with fine scale [75], and it collects information on European land. This examination provides spatial information that can be used for agricultural goals and to define the impact on the environment and natural resources. Each LUCAS point collects information including land cover, land use, and environmental parameters, identified as microdata [76]. For the calculation of crop land, LUCAS microdata was used (from class B10 to class B50). These data are available online and both are downloadable; for the year 2015 (https://ec.europa.eu/eurostat/web/lucas/data/primary-data/2015, accessed on 13 January 2022), for the year 2018 (https://ec.europa.eu/eurostat/web/lucas/data/primary-data/2018, accessed on 13 January 2022). The areas were calculated in QGIS (QGIS.org, 2021, QGIS Geographic Information System, QGIS Association. http://www.qgis.org, accessed on 13 January 2022) following Gallego and Bamps [75]. ACL, mapped by LUCAS in the Apulia region, resulted in 733,801 ha and 773,828 ha for 2015 and 2018, respectively. Subsequently, areas detected by LUCAS were mapped by using Global Land Cover [77,78] in Google Earth Engine [79]. In Global Land Cover, cultivated areas are aggregated into crop land. The separation between ACL and crop land is performed through a multitemporal analysis, by using the LANDSAT8 Collection 1 Tier 1 composite dataset (https://developers.google.com/earth-engine/datasets/catalog/LANDSAT_LC08_C01_T1_8DAY_NDVI, accessed on 13 January 2022) which allows the calculation of the averaged NDVI—using six images for 2015 and six images for 2018. This allows the creation of a mask to distinguish ACL from croplands, setting the threshold between 0.08 and 0.30 during summer periods (1 July–15 August), in which differences between these two categories are more evident in Mediterranean areas. This threshold guarantees significant difference to areas detected by LUCAS. This analysis makes it possible to map ACL areas—732,052 ha for 2015 and 772,654 ha for 2018, respectively (Figure 2), with a difference of 40,602 ha between 2015 and 2018 ACL.
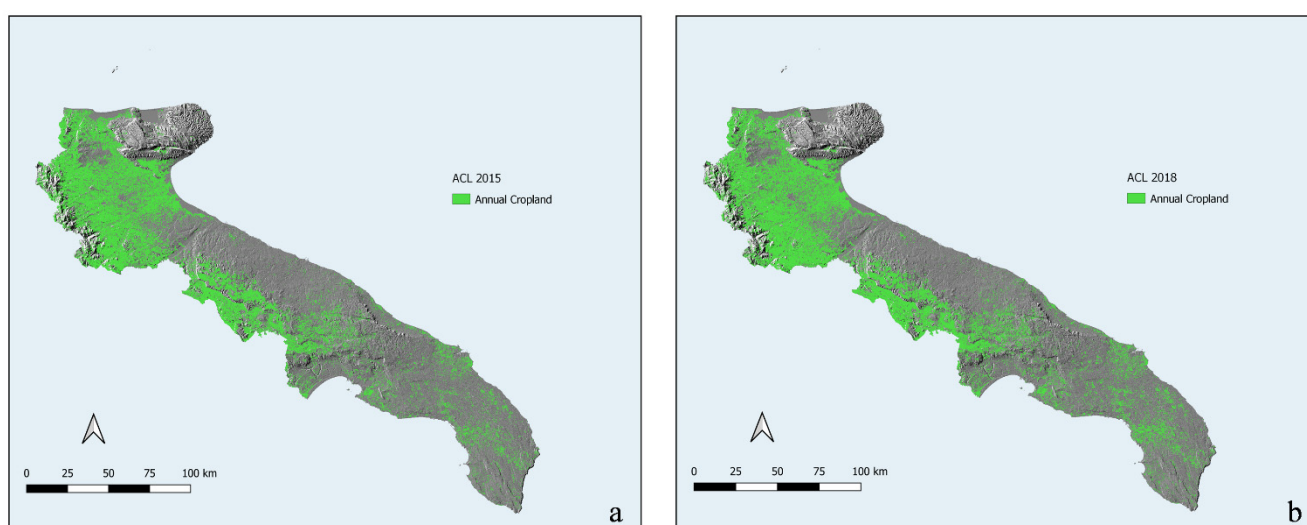

Figure 2. Annual cropland of the Apulia region in (**a**) 2015 and (**b**) 2018. Hill shade calculated using NASA DEM 30 m (https://lpdaac.usgs.gov/products/nasadem_hgtv001/, accessed on 13 January 2022).

The boundaries of the area under CA are provided by AGEA (Italian Agricultural Payments Agency), and the total area corresponds to 25,506 ha (Figure 3).
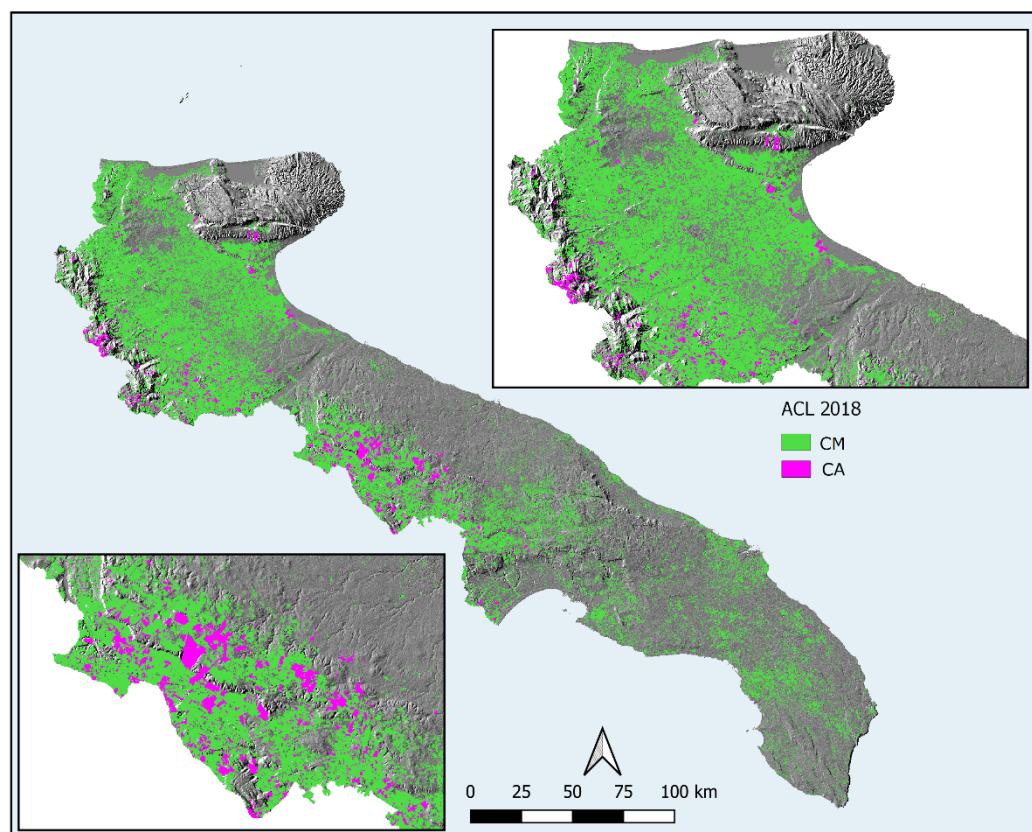

Figure 3. Annual cropland of the Apulia region in 2018 under conventional management (CM) and conservation agriculture (CA). Hill shade calculated using NASA DEM 30 m (https://lpdaac.usgs.gov/products/nasadem_hgtv001, accessed on 13 January 2022).

2.4. RUSLE Factors Multiplication

The multiplication of all the RUSLE factors was carried out in GEE, carrying all the factors to the same resolution scale, 10 m resampling, and reducing resolution for each factor by using bilinear interpolation, and with the same EPSG:3035 reference system (Figure 4). RUSLE is calculated for four consecutive annual production cycles, as shown in Table S2.
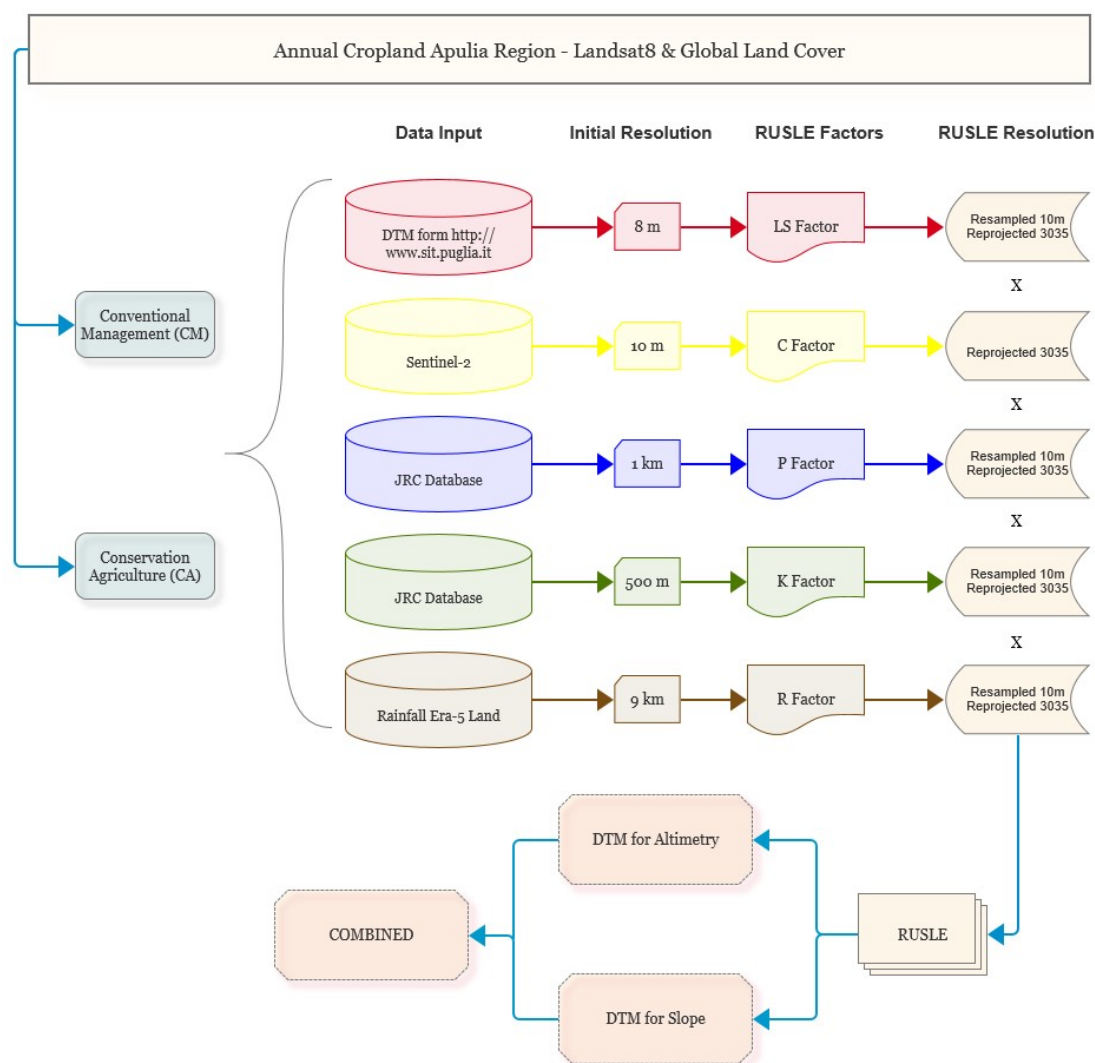
Figure 4. Methodology workflow.

For an optimal understanding of RUSLE distribution in the Apulia region, altitudes and slopes were calculated by using DTM in GEE. Altimetry was classified in three categories (according to the Italian Institute of Statistics—ISTAT, https://www.istat.it (accessed on 13 January 2022), based on their altitude above sea level: plain ($0 \leq$ altitude $\leq$ 300 m a.s.l.), hilly (300 < altitude < 800 m a.s.l.), and mountain (altitude $\geq$ 800 m a.s.l.). Each of these three categories are designated to a numerical class: 100 for the plain, 200 for the hilly, and 300 for the mountain. The slope's division in categories is carried out by dividing the slope range into three quantiles: low slope (under 1.8%), medium slope (1.8–3.7%), and high slope (over 3.3%). Each class was renominated by using a number: 1 for low slope, 2 for medium slope, and 3 for high slope. Moreover, the two categories were combined to obtain nine classes for both the scenarios (Table S3). As a final step, the statistics for each category were calculated.

3. Results and Discussion

3.1. Rainfall Erosivity (R-Factor)

The average annual *R*-factor for the Apulia region in the 1981–2019 year-period totals 318.3 MJ mm h^{-1} ha^{-1} y^{-1}, with a standard deviation of 57.4 MJ mm h^{-1} ha^{-1} y^{-1} (Table S1). If we consider all the year-periods, the annual average values of the erosive storm ranged from 198.8 to 504.2 MJ mm h^{-1} ha^{-1} y^{-1} for the 1981–2017 and 1981–2019 year periods,

respectively. The Apulia region values are more than twice lower than the average *R*-value obtained by the 1290 non-Italian stations (723 MJ mm h⁻¹ ha⁻¹ y⁻¹) contained in the Rainfall Erosivity Database on the European Scale (REDES) (Borrelli et al. [80]; Panagos et al. [81]). Considering the ACL of the Apulia region, *R*-factor ranged from 280.4 to 284.4 MJ mm h⁻¹ ha⁻¹ y⁻¹ (1981–2016 and 1981–2019, respectively) (Table S1; Figure 5). The high *R*-factor corresponds to mountain areas (Figure 5) proximity to the Daunian Sub-Apennine, in the province of Foggia in the northwest, and to the Murgia plateau in the provinces of Barletta–Andria–Trani and Bari.
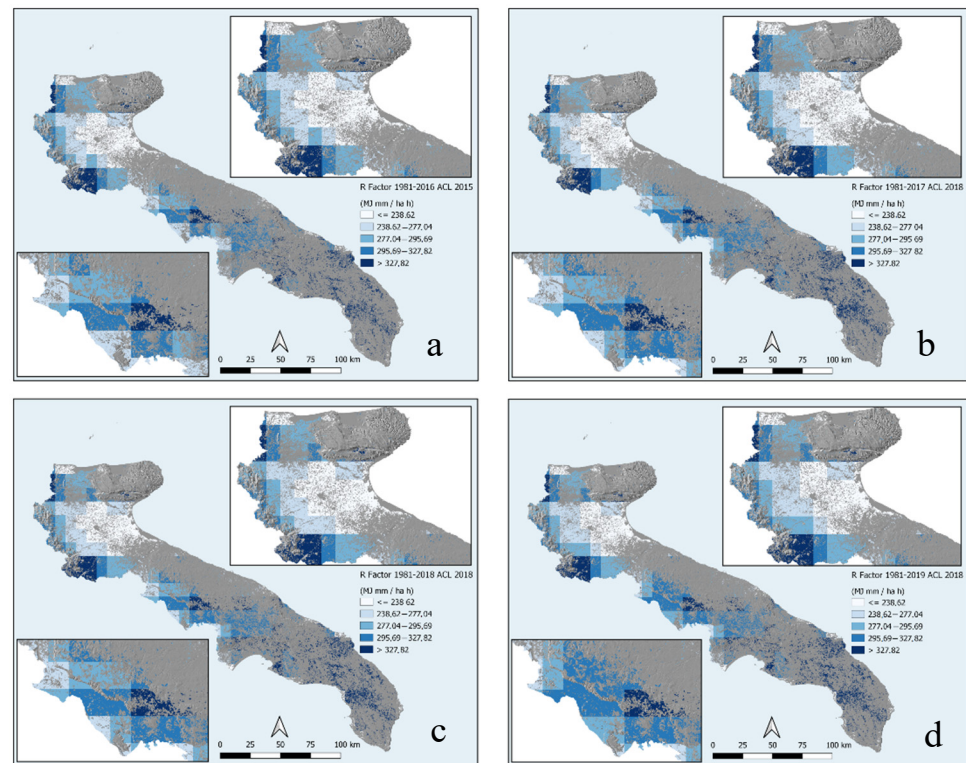
Figure 5. Maps of rainfall erosivity factor (*R*) of Apulia region with Era-5 land (9 km resolution) for the periods (**a**) 1981–2016, (**b**) 1981–2017, (**c**) 1981–2018, and (**d**) 1981–2019.

3.2. Soil Erodibility (K) and Support Practice Factor (P)

The spatial variation of K-factor values from the ESDAC dataset in the Apulia region depend on the variation of ACL area for both years. The results showed a mean value of 0.0331 t ha h ha⁻¹ MJ⁻¹ mm⁻¹ for 2015 (Figure 6a) and 0.0329 t ha h ha⁻¹ MJ⁻¹ mm⁻¹ for 2018 (Figure 6b).

Figure 6. Soil erodibility factor (*K*) maps of the Apulia region for annual cropland in (**a**) 2015 and (**b**) 2018.

In both years, the highest value of *K*-factor is distributed in the areas of Tavoliere and in the Daunian Sub-Apennine, in the province of Foggia in the northwest, and in the Murgia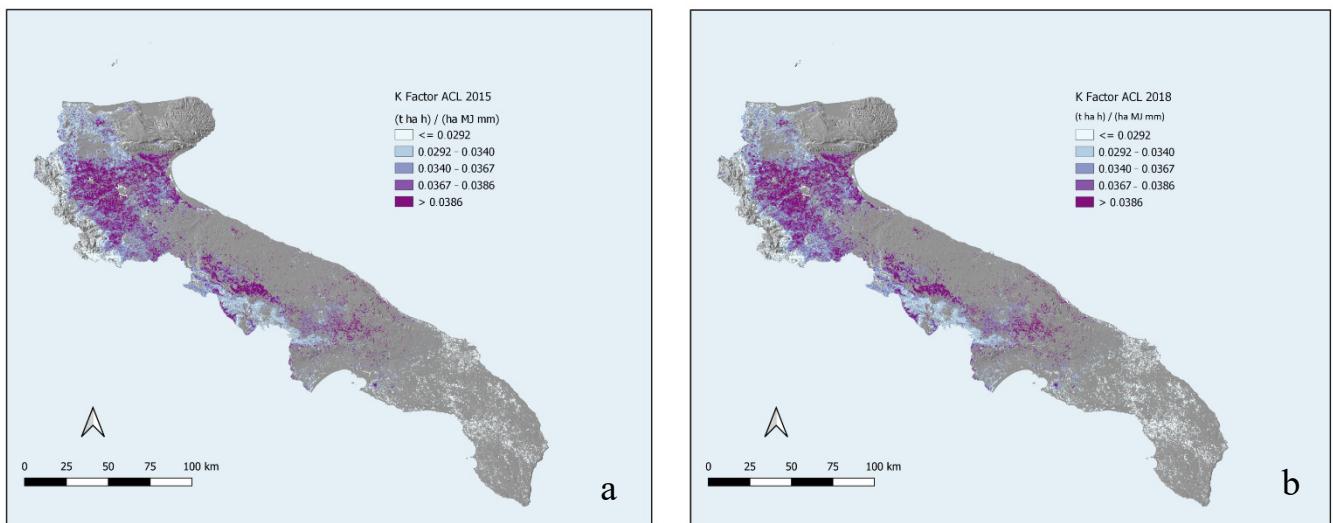 plateau in the provinces of Barletta–Andria–Trani and Bari. From the ESDAC dataset for the P-factor, it was possible to extrapolate factors for the ACL area for both years. The P-mean for 2015 is 0.8736, and for 2018, 0.8682. In both maps (Figure 7), the higher values are found in the mountainous regions where the CA system is mainly applied.
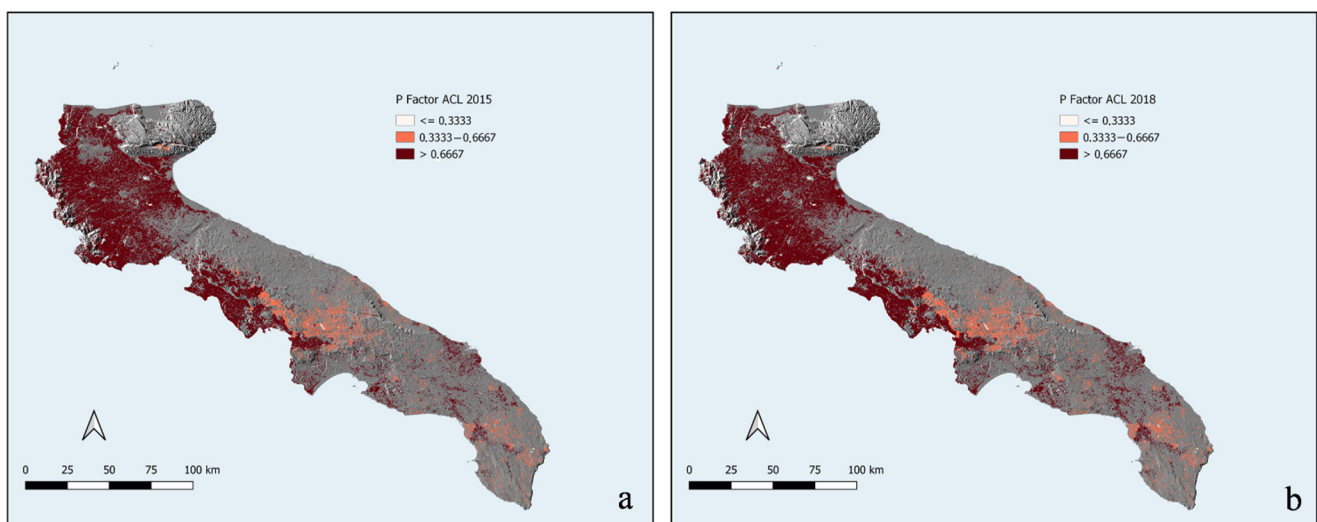

Figure 7. Support practice factor (*P*) maps of the Apulia region for annual cropland in (**a**) 2015 and (**b**) 2018.

3.3. Topographic Factor (LS)

LS-factor is calculated for the ACL of the Apulia region. The averaged values (Figure 8) are 0.93 and 0.88 for 2015 and 2018, respectively.
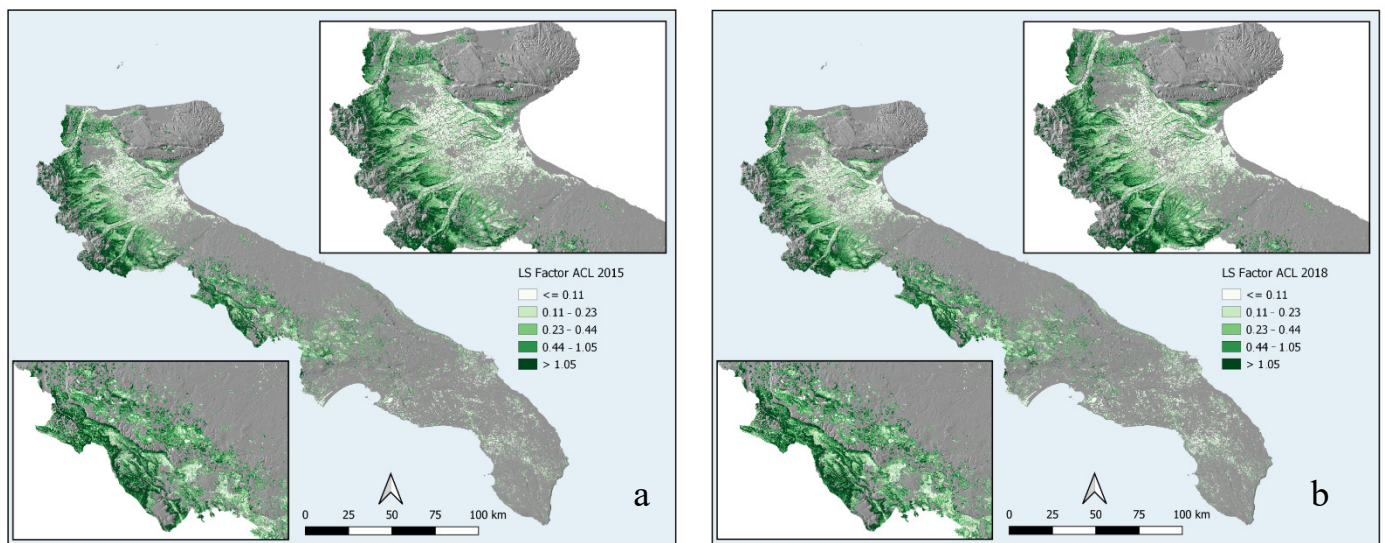
Figure 8. Slope length and steepness (*LS*) factor map of the Apulia region for annual cropland in (**a**) 2015 and (**b**) 2018.

The high *LS* values are found in the mountainous area with steep topography, especially in the west where mountains are prevalent (Daunian Sub-Apennine and Murgia), while the lowest values are distributed along the Adriatic and Ionic coasts. To determine the spatial resolution (cell size) of the soil erosion model results, and, therefore, to incorporate the soil erosion potential due to surface runoff, we used a high-resolution (8 m) DTM of the Apulia region to calculate *LS*-factor. This resolution of Apulia region DTM is the best available at regional scale. Generally, the DTM resolutions used on a European scale are in the range of 25 to 100 m [56], while at regional scale, the resolutions range from 5 m to 40 m [82,83]. As reported by Bircher et al. [84], several authors have mentioned the importance of assessing the risk of soil erosion based on the size of the cells and the accuracy of the DTM. The risk that can occur is that a low DTM resolution (large cells) is not able to map relevant topographic details [85–87].

3.4. Cover-Management (C-Factor)

The four-year mean for the *C*-factor values of the two management systems is shown separately for each year and crop stage in Table 1. The four-year mean *C*-factor for CM in ACL of the Apulia region is 0.2867, while for the CA it is 0.2745, with an average percentage reduction of the *C*-factor of 4.2% according to the cropping system adopted. The lowest *C*-factor values for CM and CA were registered both in the year 2019/2020 (0.2656 and 0.2552, respectively), while the highest were in the year 2016/2017 (0.3268 and 0.3122, respectively; Supplementary Figures S1 and S2). The four-cropping cycle average of NDVI for the study site varied from 0.3653 to 0.4078 (in 2016/2017 and 2019/2020, respectively) with an average over 0.3928. The ground-cover percentage was directly measured in all ACL with 10 m resolution. Based on the two management systems in the study area, higher *C*-values were observed in the CM management system, thus indicating higher potentiality for soil erosion risk in these areas (Figure 9). Spatiotemporal dynamics are required to understand impacts and risks at regional scale. For this reason, it is necessary to identify the agricultural area that can be most affected by soil erosion by water and identify, where possible, which CA system will reduce these processes.
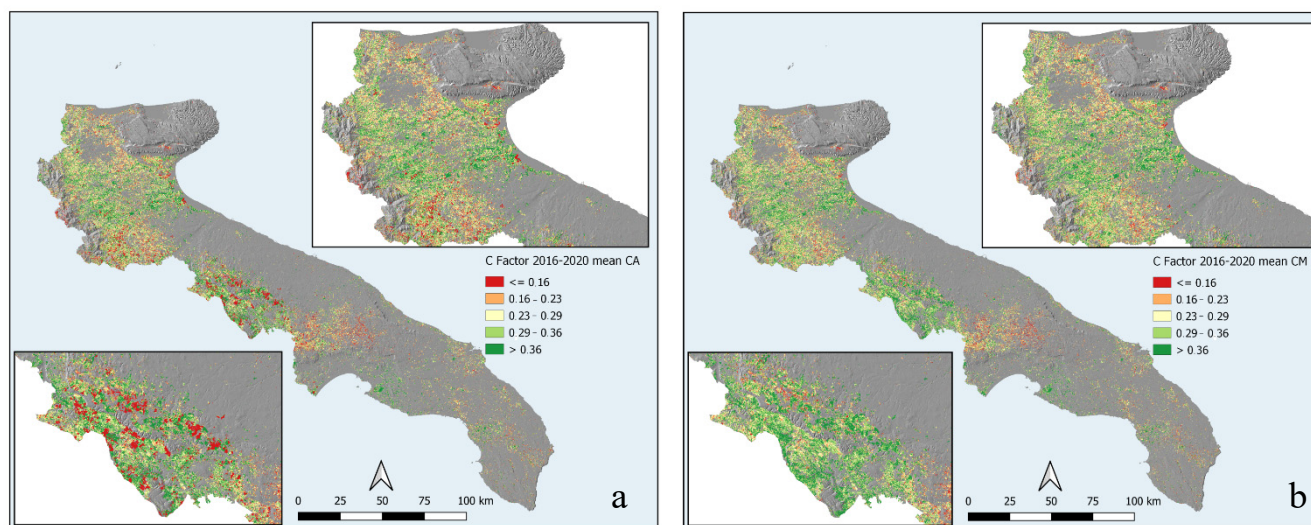
Figure 9. Cover and management (*C*) factor average maps (2016–2020) of the Apulia region under (**a**) conventional management and (**b**) conservation agriculture for annual cropland.

Our approach was focused on the use of multitemporal satellite images to capture the temporal variability of the determination of factor *C*. This approach is used for ecosystem modeling studies on a large scale [34,88] and places the focus on the importance of explicit consideration of temporal variability on soil management systems to protect agricultural land from the impact of soil erosion by water [89]. Generally, in large-scale modeling applications, the estimation of multiple sub-factor *C* parameters is derived from pre-existing literature [34,89,90] and does not use spatially explicit land-cover data for the determination of the *C*-factor; it is, rather, based on statistical data. Current approaches on a European scale adopt the CORINE Land Cover Database for the calculation of the *C*-factor [12]. This data is inadequate in its spatial and thematic resolution compared to RS sensors with up-to-date information on proximal measures of vegetation, which is a key aspect for a correct and accurate calculation of *C*-factor [22]. This aspect becomes even more important for areas where the spatial and temporal dynamics of the vegetation cover are provided by the cultivation of crops [83,91]. On the other hand, data obtained from field experiments carried out to measure the values of the *C*-factor take a long time and are rarely available [22].

Within this work, by using a spatial resolution of 10 m (obtained through Sentinel 2A) and applying the formula proposed by Van der Knijff et al. [12] integrated with that of Panagos et al. [34], we obtained a more detailed resolution on the ACL (previously mapped) to multitemporal NDVI calculation. This NDVI-derived method can variably capture the actual soil cover status [82] rather than using aggregate and fixed data over time. This approach can be useful in increasing the accuracy of the calculation of the *C*-factor [67,92,93]. Our results show how, for the estimation of the *C*-factor in the Apulia region, the values are comparable to those present in the literature for ACL [67,74,94,95], which fluctuate between 0.01 and 0.44 for ACL, but with a much more accurate regional scale of detail. Concerning the difference between the CM and CA systems, our results demonstrate how, on average, the adoption of CA reduces the *C*-factor by 4.2% in line with other analyzed scenarios [34]. CA has been reported in many studies as an effective strategy to control erosion processes, maintain soil fertility, increase soil carbon sequestration, and improve cropping system sustainability [96–98].

3.5. Soil Loss Estimation in the Apulia Region

3.5.1. Loss Rates

The loss rates (A), in t ha^{-1} y^{-1}, for the Apulia region in this study are generated by using the RUSLE model to calculate the mean for the 2016–2020 period. The results are shown in Table 2. The four-year agricultural annual crop cycle average for CM is 2.28 t ha^{-1} y^{-1}, while for CA it is 2.11 t ha^{-1} y^{-1} (Figure 10).

Table 2. RUSLE values for the 2016–2020 period in the Apulia region for each management system.

	RUSLE		
	CM	CA	
Agricultural Seasons 2016–2020	t ha^{-1}	t ha^{-1}	Δ%
Mean	2.28	2.11	−7.5

CM = conventional management. CA = conservation agriculture. RUSLE = Revised Universal Soil Loss Equation. Δ% = percentage difference.
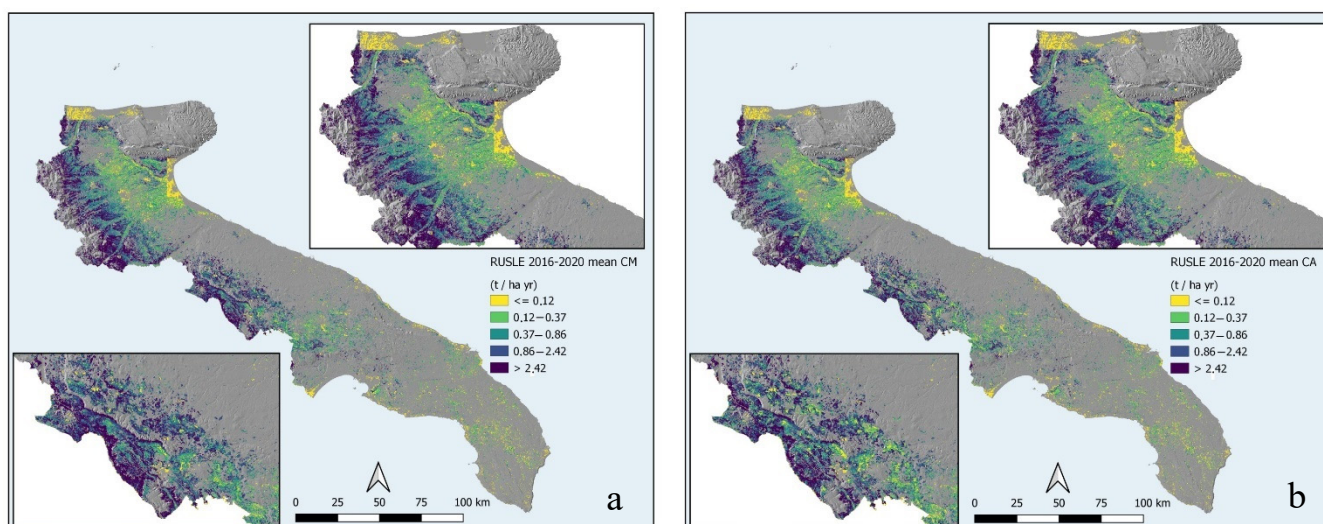

Figure 10. RUSLE model average maps (2016–2020) in Apulia region under (**a**) conventional management and (**b**) conservation agriculture for annual cropland.

Moreover, for the intermediate RUSLE calculation, the lower and higher values for CM system are 2.02 and 2.69 t ha^{-1} y^{-1}, while for CA system, are 1.88 and 2.49 t ha^{-1} y^{-1} for the two-year periods 2019/2020 and 2016/2017, respectively. These patterns are shown in Supplementary Figures S3 and S4 and Table S4.

Interestingly, the areas featuring high risk of soil erosion are in the Tavoliere and in the Daunian Sub-Apennine, in the northwest, as well as in the Murgia plateau in the center of the Apulia region. As for the soils under CA, there is instead a reduction in soil erosion risk in the same areas as well as in the south of the Apulia region (Salento, province of Lecce).

Current results from the RUSLE model reveal a serious soil erosion risk where the CM system is adopted, while the CA system showed a trend over the years to contain the rate of soil loss for ACL in the Apulia region, representative of pedoclimatic conditions widely present in large agricultural areas of the Mediterranean basin. As suggested by Wischmeier and Smith [52], practices of improved tillage, such as no-till and cover crops, were considered as conservation cropping and management practices and implemented in the *C*-factor. A recent scenario analysis carried out on 54 countries, that reported information on the implementation of CA to the Food and Agriculture Organization of United

Nations (FAO), assumes a 45% reduction of soil erosion risk in CA compared to CM [99]. Furthermore, a previous study by Borrelli et al. [100] shows how in Italy, when good agricultural and environmental conditions (GAEC) including CA are adopted, there is a potential to reduce erosion by 8.5%, while for the Apulia region, the potential rate of erosion is 5%. The results obtained (Table 2) at this territorial scale are in line with this scenario and, moreover, by improving the spatial resolution of DTM (8 m), the erosion rate calculated over the four years (2016–2020) shows an average of 7%, in line with the scenario assumed for the Apulia region.

3.5.2. Mean Loss Rates for Altitude and Slope Classes

RUSLE values were calculated for altimetric and slope classes for each agricultural annual crop cycle (Table 3).

Table 3. RUSLE calculation for each altitude and slope class and their combination of the two management systems in four years in the Apulia region. CM = conventional management. CA = conservation agriculture. RUSLE = Revised Universal Soil Loss Equation. Δ% = percentage difference.

			RUSLE													
Agricultural Seasons ➝			2016–2017					2017–2018			2018–2019			2019–2020		
		Total Annual Crops Area 2015	CM	CA	Δ%	Total Annual Crops Area 2018	CM	CA	Δ%	CM	CA	Δ%	CM	CA	Δ%	Means Δ%
Numerical Class	Altitude Class	%	t ha⁻¹ y⁻¹	t ha⁻¹ y⁻¹	%	%	t ha⁻¹ y⁻¹	t ha⁻¹ y⁻¹	%	t ha⁻¹ y⁻¹	t ha⁻¹ y⁻¹	%	t ha⁻¹ y⁻¹	t ha⁻¹ y⁻¹	%	%
100	Plain	67.56	1.57	1.50	−4.5	68.23	1.14	1.09	−4.4	1.35	1.32	−2.2	1.31	1.26	−3.8	−3.7
200	Hilly	31.86	4.03	3.63	−9.9	31.33	2.78	2.51	−9.7	3.55	3.15	−11.3	2.91	2.63	−9.6	−10.1
300	Mountain	0.58	4.89	4.01	−18	0.44	2.72	2.45	−9.9	2.82	2.88	2.1	2.92	2.63	−9.9	−8.9
1	Low slope	29.25	0.64	0.61	−4.7	29.79	0.45	0.42	−6.7	0.55	0.53	−3.6	0.53	0.51	−3.8	−4.7
2	Medium slope	33.50	0.79	0.75	−5.1	34.15	0.55	0.52	−5.5	0.68	0.65	−4.4	0.64	0.61	−4.7	−4.9
3	High slope	37.25	3.80	3.50	−7.9	35.99	2.69	2.49	−7.4	3.32	3.06	−7.8	2.92	2.71	−7.2	−7.6
101	Plain + low slope	24.67	0.65	0.63	−3.1	25.19	0.56	0.55	−1.8	0.66	0.57	−13.6	0.57	0.56	−1.8	−5.1
102	Plain + medium slope	24.93	0.79	0.77	−2.5	25.47	0.47	0.45	−4.3	0.56	0.57	1.8	0.57	0.56	−1.8	−1.7
103	Plain + high slope	17.94	3.10	2.96	−4.5	17.54	1.98	1.90	−4	2.37	2.27	−4.2	2.24	2.15	−4	−4.2
201	Hilly + low slope	4.51	1.07	0.97	−9.3	4.60	0.78	0.71	−9	1.08	0.77	−28.7	0.74	0.67	−9.5	−14.1
202	Hilly + medium slope	8.56	1.31	1.18	−9.9	8.68	0.82	0.74	−9.8	1.12	0.90	−19.6	0.86	0.78	−9.3	−12.2
203	Hilly + high slope	18.75	5.66	5.11	−9.7	18.03	3.67	3.31	−9.8	4.67	4.17	−10.7	3.84	3.48	−9.4	−9.9
301	Mountain + low slope	0.00	1.21	0.88	−27.3	0.00	1.28	1.05	−18	1.25	1.12	−10.4	1.34	1.08	−19.4	−18.8
302	Mountain + medium slope	0.01	1.43	1.11	−22.4	0.01	0.46	0.40	−13	0.49	0.47	−4.1	0.50	0.43	−14	−13.4
303	Mountain + high slope	0.56	5.89	4.84	−17.8	0.43	2.74	2.47	−9.9	2.85	2.90	1.8	2.94	2.65	−9.9	−8.9

The erosion rate is variable across the regional territory because the pedological and climatic variability is high, but even more so is the morphology of the Apulia region, which is also found in the discontinuous adoption of CA. In the Apulia region, the ACL lying on plain (0 ≤ 300 m a.s.l.) and hilly (300 m < 800 m a.s.l.) areas covers 99% of the surfaces, and about 36% of the study areas is located on slopes greater than 3.7%. In our study, with the introduction of the CA management system, the soil loss rate in these areas ranged from −1.7% for the plain + medium slope terrain to −18.8% for the mountain + low slope terrain, with an overall average of all terrain classes considered, during the four years, of −8.5%.

In the plains, 68% of the total ACL is present, and in four years, the contribution of CA can reduce the soil loss rate by −3.7%, compared to the CM system. For the hilly areas (32% of the total ACL), the erosion rate decreases by −10.1% when CA is adopted. ACL distributed in the slope classes are very similar, and the contribution of CA is higher on the high slopes, decreasing the erosion rate by −7.6% compared with the CM system, according to the scenario analysis for Italy by Borrelli et al. [100].

3.5.3. Combination of Altitude and Slope Classes

In the combination of altitude and slope classes, the highest effect is on the hilly + low slope and hilly + medium slope. The CA management system contributes, respectively, −14.1% and −12.2% to the erosion rate over the four years, compared with CM. These values are in line with the scenario proposed by Panagos et al. [101], in which a projection of soil loss by water erosion in Europe by 2050 is calculated, and it is reported that there will be a potential of reduction of soil losses of 17–22% with the contribution of reduced tillage combined with cover crops. This scenario is confirmed by the results of Table 3, in which the highest absolute values of soil loss rate containment are obtained for the altitude and slope classes in which CA is currently marginally adopted.

4. Conclusions

Soil erosion is among the most critical environmental hazards of modern times. Vast areas of Mediterranean land now being cultivated with CM may be rendered unproductive, or at least economically unproductive, if erosion continues unabated. Soils cultivated with annual crops in Mediterranean climatic conditions under conservative agriculture can benefit from a permanent cover for the direct increase of surface water infiltration, significantly reducing surface runoff and therefore soil erosion risk.

In order to estimate soil loss rate at regional scale, empirical models are accurate and easy to interpret and require modest resources. They can be processed with readily available inputs to identify areas exposed to high risk of erosion. In this study, RUSLE models integrated with GEE and QGIS were used to estimate soil loss rate on the ACL of the Apulia region for a period of four annual crop cycles—from 2016 to 2020—for both the scenarios.

Results show that where the CA system is applied continuously in ACL, there is an annual average reduction of soil loss rate over 7% compared with CM; furthermore, it is significatively different for altimetric, slope, and combined classes, showing that the important contribution of the CA system can reduce soil loss rate in hilly areas by 10.1% and in hilly + low slope terrain by 14.1%. These results represent a baseline to estimate the effects of the adoption of the specific agro-environment-climate measure on soil erosion risk during the first phase of transition from conventional to conservation management systems. Consequently, the results of this study can represent an objective target baseline for the planning of the new CAP 2023–2027, which provides for the selection of reliable concrete and achievable result indicators, including erosion by water, whose values can be monitored and verified periodically. The goal is to increase the agricultural area under CA in the Apulia region and in those areas with semiarid Mediterranean climate where there is greater loss of soil due to water erosion. Such data, which should be monitored periodically, could be used to evaluate soil conservation management planning processes, and help determine the dimension and duration of a transition phase to support farmers in providing ecosystem restoration services, reduction of erosion by water, and improvement of soil healthy and agricultural productivity.

management for annual cropland; Figure S4: Soil loss rate using RUSLE model for Apulia region under conservation agriculture for annual cropland; Table S1: Descriptive statistical values of the *R* factor (MJ mm h⁻¹ ha⁻¹ y⁻¹) for each year-periods of RUSLE calculation; Table S2: Calculation of annual cropland areas in Apulia region in four different years; Table S3: Nine new classes obtained by combined altitude class with three quantiles; Table S4: Intermediate RUSLE values in the Apulia region for each management system.

Author Contributions: Conceptualization: M.P. (Matteo Petito), S.C., G.P., F.D., B.P., and M.P. (Michele Pisante); methodology: M.P. (Matteo Petito), S.C., G.P., and F.D.; software: M.P. (Matteo Petito) and B.P.; formal analysis: M.P. (Matteo Petito), S.C., and B.P.; resources: F.D. and M.P. (Michele Pisante); data curatio[n: M.P. (Matteo Petito), S.C., G.P., and M.P. (Michele Pisante); writing—original draft: M.P. (Matteo Petito), S.C., and G.P.; funding acquisition: M.P. (Michele Pisante); writing—review and editing: M.P. (Michele Pisante). All authors have read and agreed to the published version of the manuscript.

Institutional Review Board Statement: Not applicable.

Informed Consent Statement: Not applicable.

Data Availability Statement: The authors confirm that the data supporting the findings of this study are available within the article and its Supplementary Materials.

Conflicts of Interest: The authors declare that they have no known competing financial interests or personal relationships that could have appeared to influence the work reported in this paper.

References

1. de la Rosa, D.; Sobral, R. Soil Quality and Methods for its Assessment. In *Land Use and Soil Resources*; Braimoh, A.K., Vlek, P.L.G., Eds.; Springer: Dordrecht, Netherlands, 2008; pp. 167–200, ISBN 978-1-4020-6778-5.
2. Pham, T.G.; Nguyen, H.T.; Kappas, M. Assessment of soil quality indicators under different agricultural land uses and topographic aspects in Central Vietnam. *Int. Soil Water Conserv. Res.* **2018**, *6*, 280–288. https://doi.org/10.1016/j.iswcr.2018.08.001.
3. Tian, P.; Zhu, Z.; Yue, Q.; He, Y.; Zhang, Z.; Hao, F.; Guo, W.; Chen, L.; Liu, M. Soil erosion assessment by RUSLE with improved P factor and its validation: Case study on mountainous and hilly areas of Hubei Province, China. *Int. Soil Water Conserv. Res.* **2021**, *9*, 433–444. https://doi.org/10.1016/j.iswcr.2021.04.007.
4. Bullock, P. CLIMATE CHANGE IMPACTS. In *Encyclopedia of Soils in the Environment*; Hillel, D., Ed.; Elsevier: Oxford, UK, 2005; pp. 254–262, ISBN 978-0-12-348530-4.
5. Karlen, D.L.; Mausbach, M.J.; Doran, J.W.; Cline, R.G.; Harris, R.F.; Schuman, G.E. Soil Quality: A Concept, Definition, and Framework for Evaluation (A Guest Editorial). *Soil Sci. Soc. Am. J.* **1997**, *61*, 4–10. https://doi.org/10.2136/sssaj1997.03615995006100010001x.
6. Lal, R. *Soil Quality and Soil Erosion*; Lal, R., Ed.; CRC Press: Boca Raton, FL, USA, 2018; ISBN 9780203739266.
7. Pimentel, D. Soil Erosion: A Food and Environmental Threat. *Environ. Dev. Sustain.* **2006**, *8*, 119–137. https://doi.org/10.1007/s10668-005-1262-8.
8. Nyakatawa, E.; Jakkula, V.; Reddy, K.; Lemunyon, J.; Norrisjr, B. Soil erosion estimation in conservation tillage systems with poultry litter application using RUSLE 2.0 model. *Soil Tillage Res.* **2007**, *94*, 410–419. https://doi.org/10.1016/j.still.2006.09.003.
9. Dale, V.H.; Polasky, S. Measures of the effects of agricultural practices on ecosystem services. *Ecol. Econ.* **2007**, *64*, 286–296. https://doi.org/10.1016/j.ecolecon.2007.05.009.
10. Dominati, E.; Patterson, M.; Mackay, A. A framework for classifying and quantifying the natural capital and ecosystem services of soils. *Ecol. Econ.* **2010**, *69*, 1858–1868. https://doi.org/10.1016/j.ecolecon.2010.05.002.
11. Onori, F.; De Bonis, P.; Grauso, S. Soil erosion prediction at the basin scale using the revised universal soil loss equation (RUSLE) in a catchment of Sicily (southern Italy). *Environ. Geol.* **2006**, *50*, 1129–1140. https://doi.org/10.1007/s00254-006-0286-1.
12. Van der Knijff, J.M.; Jones, R.J.A.; Montanarella, L. *Soil Erosion Risk Assessment in Europe*; EUR 19044 EN; Office for Official Publications of the European Communities: Luxemburg, 2000.
13. McCool, D.K.; Williams, J.D. Soil Erosion by Water. In *Encyclopedia of Ecology*; Jørgensen, S.E., Fath, B.D., Eds.; Academic Press: Oxford, UK, 2008; pp. 3284–3290, ISBN 978-0-08-045405-4.

14. Stolte, J.; Tesfai, M.; Øygarden, L.; Kværnø, S; Keizer, J.; Verheijen, F. *Soil Threats in Europe: Status, Methods, Drivers and Effects on Ecosystem. Services: Deliverable 2.1 RECARE Project*; European Soil Data Centre, European Union, 2016. Available online: https://esdac.jrc.ec.europa.eu/public_path/shared_folder/doc_pub/EUR27607.pdf (accessed on 13 January 2022).

15. Paul, C.; Kuhn, K.; Steinhoff-Knopp, B.; Weißhuhn, P.; Helming, K. Towards a standardization of soil-related ecosystem service assessments. *Eur. J. Soil Sci.* **2021**, *72*, 1543–1558. https://doi.org/10.1111/ejss.13022.

16. Steinhoff-Knopp, B.; Kuhn, T.K.; Burkhard, B. The impact of soil erosion on soil-related ecosystem services: Development and testing a scenario-based assessment approach. *Environ. Monit. Assess.* **2021**, *193*, 274. https://doi.org/10.1007/s10661-020-08814-0.

17. Farooq, M.; Pisante, M. *Innovations in Sustainable Agriculture*; Farooq, M., Pisante, M., Eds.; Springer International Publishing: Cham, Switzerland, 2019; ISBN 978-3-030-23168-2.

18. Füssel, H.M., Marx, A., Hildén, M. *Climate Change, Impacts and Vulnerability in Europe 2016—An Indicator-based Report*; EEA Report No 1/2017; EEA: Copenhagen, Denmark, 2017.

19. Jat, R.A.; Kanwar L.; Sahrawat Amir, H.; Kassam, T.F. Conservation agriculture for sustainable and resilient agriculture: Global status, prospects and challenges. In *Conservation Agriculture: Global Prospects and Challenges*; CABI Publishing: Wallingford, UK, 2014; pp. 1–25.

20. Ronco, P.; Zennaro, F.; Torresan, S.; Critto, A.; Santini, M.; Trabucco, A.; Zollo, A.L.; Galluccio, G.; Marcomini, A. A risk assessment framework for irrigated agriculture under climate change. *Adv. Water Resour.* **2017**, *110*, 562–578. https://doi.org/10.1016/j.advwatres.2017.08.003.

21. Ferreira, C.S.S.; Seifollahi-Aghmiuni, S.; Destouni, G.; Ghajarnia, N.; Kalantari, Z. Soil degradation in the European Mediterranean region: Processes, status and consequences. *Sci. Total Environ.* **2022**, *805*, 150106. https://doi.org/10.1016/j.scitotenv.2021.150106.

22. Preiti, G.; Romeo, M.; Bacchi, M.; Monti, M. Soil loss measure from Mediterranean arable cropping systems: Effects of rotation and tillage system on C-factor. *Soil Tillage Res.* **2017**, *170*, 85–93. https://doi.org/10.1016/j.still.2017.03.006.

23. Montanarella, L. *Soil Conservation in the European Union*; DLG-Verlag GmbH: Frankfurt, Germany, 2013.

24. Morgan, R.P. *Soil Erosion and Conservation*; John Wiley & Sons: Hoboken, NJ, USA; 2005; ISBN 978-1-405-14467-4.

25. Simonneaux, V.; Cheggour, A.; Deschamps, C.; Mouillot, F.; Cerdan, O.; Le Bissonnais, Y. Land use and climate change effects on soil erosion in a semi-arid mountainous watershed (High Atlas, Morocco). *J. Arid Environ.* **2015**, *122*, 64–75. https://doi.org/10.1016/j.jaridenv.2015.06.002.

26. Bhatt, R.; Kukal, S.S.; Busari, M.A.; Arora, S.; Yadav, M. Sustainability issues on rice–wheat cropping system. *Int. Soil Water Conserv. Res.* **2016**, *4*, 64–74. https://doi.org/10.1016/j.iswcr.2015.12.001.

27. Corsi, S.; Friedrich, T.; Kassam, A.; Pisante, M.; Sà, J.D.M. *Soil Organic Carbon Accumulation and Greenhouse Gas Emission Reductions from Conservation Agriculture: A Literature Review*; Food and Agriculture Organization of the United Nations: Rome, Italy, 2012; Volume 16, ISBN 9789251071878.

28. González-Sánchez, E.J.; Moreno-García, M., Kassam, A.; Holgado-Cabrera, A.; Triviño-Tarradas, P.; Carbonell-Bojollo, R.; Pisante, M.; Veroz-González, O.; Basch, G. *Conservation Agriculture: Making Climate Change Mitigation and Adaptation Real in Europe*; European Conservation Agriculture Federation: Brussels, Belgium, 2017.

29. Kassam, A. *Advances in Conservation Agriculture: Volume 2: Practice and Benefits.*; Kassam, A., Ed.; Burleigh Dodds Science Publishing Limited: Cambridge, UK, 2020.

30. Pisante, M.; Stagnari, F.; Acutis, M.; Bindi, M.; Brilli, L.; Di Stefano, V.; Carozzi, M. Conservation Agriculture and Climate Change. In *Conservation Agriculture*; Springer International Publishing: Cham, Switzerland, 2015; pp. 579–620.

31. Sturny, W.G.; Chervet, A.; Maurer-Troxler, C.; Ramseier, L.; Müller, M.; Schafflützel, R.; Richner, W.; Streit, B.; Weisskopf, P.; Zihlmann, U. Comparison of no-tillage and conventional plow tillage—A synthesis. *AGRARForschung* **2007**, *14*, 350–357.

32. Panagos, P.; Ballabio, C.; Poesen, J.; Lugato, E.; Scarpa, S.; Montanarella, L.; Borrelli, P. A Soil Erosion Indicator for Supporting Agricultural, Environmental and Climate Policies in the European Union. *Remote Sens.* **2020**, *12*, 1365. https://doi.org/10.3390/rs12091365.

33. Cerdan, O.; Govers, G.; Le Bissonnais, Y.; Van Oost, K.; Poesen, J.; Saby, N.; Gobin, A.; Vacca, A.; Quinton, J.; Auerswald, K.; et al. Rates and spatial variations of soil erosion in Europe: A study based on erosion plot data. *Geomorphology* **2010**, *122*, 167–177. https://doi.org/10.1016/j.geomorph.2010.06.011.

34. Panagos, P.; Borrelli, P.; Meusburger, K.; Alewell, C.; Lugato, E.; Montanarella, L. Estimating the soil erosion cover-management factor at the European scale. *Land Use Policy* **2015**, *48*, 38–50. https://doi.org/10.1016/j.landusepol.2015.05.021.

35. Efthimiou, N.; Psomiadis, E. The Significance of Land Cover Delineation on Soil Erosion Assessment. *Environ. Manage.* **2018**, *62*, 383–402. https://doi.org/10.1007/s00267-018-1044-3.

36. Frattaruolo, F.; Pennetta, L.; Piccarreta, M. Desertification Vulnerability Map of Tavoliere, Apulia (Southern Italy). *J. Maps* **2009**, *5*, 117–125. https://doi.org/10.4113/jom.2009.1050.

37. Ladisa, G.; Todorovic, M.; Trisorio Liuzzi, G. A GIS-based approach for desertification risk assessment in Apulia region, SE Italy. *Phys. Chem. Earth Parts A/B/C* **2012**, *49*, 103–113. https://doi.org/10.1016/j.pce.2011.05.007.

38. Wang, H.; Zhao, H. Dynamic Changes of Soil Erosion in the Taohe River Basin Using the RUSLE Model and Google Earth Engine. *Water* **2020**, *12*, 1293. https://doi.org/10.3390/w12051293.

39. Di Nunno, F.; Granata, F. Groundwater level prediction in Apulia region (Southern Italy) using NARX neural network. *Environ. Res.* **2020**, *190*, 110062. https://doi.org/10.1016/j.envres.2020.110062.

40. Serio, F.; Miglietta, P.P.; Lamastra, L.; Ficocelli, S.; Intini, F.; De Leo, F.; De Donno, A. Groundwater nitrate contamination and agricultural land use: A grey water footprint perspective in Southern Apulia Region (Italy). *Sci. Total Environ.* **2018**, *645*, 1425–1431. https://doi.org/10.1016/j.scitotenv.2018.07.241.

41. Abu Hammad, A. Watershed erosion risk assessment and management utilizing revised universal soil loss equation-geographic information systems in the Mediterranean environments. *Water Environ. J.* **2011**, *25*, 149–162. https://doi.org/10.1111/j.1747-6593.2009.00202.x.

42. Prasannakumar, V.; Shiny, R.; Geetha, N.; Vijith, H. Spatial prediction of soil erosion risk by remote sensing, GIS and RUSLE approach: A case study of Siruvani river watershed in Attapady valley, Kerala, India. *Environ. Earth Sci.* **2011**, *64*, 965–972. https://doi.org/10.1007/s12665-011-0913-3.

43. Yesuph, A.Y.; Dagnew, A.B. Soil erosion mapping and severity analysis based on RUSLE model and local perception in the Beshillo Catchment of the Blue Nile Basin, Ethiopia. *Environ. Syst. Res.* **2019**, *8*, 17. https://doi.org/10.1186/s40068-019-0145-1.

44. Haregeweyn, N.; Tsunekawa, A.; Poesen, J.; Tsubo, M.; Meshesha, D.T.; Fenta, A.A.; Nyssen, J.; Adgo, E. Comprehensive assessment of soil erosion risk for better land use planning in river basins: Case study of the Upper Blue Nile River. *Sci. Total Environ.* **2017**, *574*, 95–108. https://doi.org/10.1016/j.scitotenv.2016.09.019.

45. Elnashar, A.; Wang, L.; Wu, B.; Zhu, W.; Zeng, H. Synthesis of global actual evapotranspiration from 1982 to 2019. *Earth Syst. Sci. Data* **2021**, *13*, 447–480. https://doi.org/10.5194/essd-13-447-2021.

46. Tian, F.; Wu, B.; Zeng, H.; Zhang, X.; Xu, J. Efficient Identification of Corn Cultivation Area with Multitemporal Synthetic Aperture Radar and Optical Images in the Google Earth Engine Cloud Platform. *Remote Sens.* **2019**, *11*, 629. https://doi.org/10.3390/rs11060629.

47. Zeng, H.; Wu, B.; Wang, S.; Musakwa, W.; Tian, F.; Mashimbye, Z.E.; Poona, N.; Syndey, M. A Synthesizing Land-cover Classification Method Based on Google Earth Engine: A Case Study in Nzhelele and Levhuvu Catchments, South Africa. *Chin. Geogr. Sci.* **2020**, *30*, 397–409. https://doi.org/10.1007/s11769-020-1119-y.

48. Renard, K.G.; Foster, G.R.; Weesies, G.A.; Porter, J.P. RUSLE: Revised universal soil loss equation. *J. Soil Water Conserv.* **1991**, *46*, 30–33.

49. Renard, K.G. *Predicting Soil Erosion by Water: A Guide to Conservation Planning with the Revised Universal Soil Loss Equation (RUSLE)*; United States Department of Agriculture: Washington, DC, USA, 1997.

50. Brown, L.C.; Foster, G.R. storm Erosivity Using Idealized Intensity Distributions. *Trans. ASAE* **1987**, *30*, 379–386. https://doi.org/10.13031/2013.31957.

51. Diodato, N. Estimating RUSLE's rainfall factor in the part of Italy with a Mediterranean rainfall regime. *Hydrol. Earth Syst. Sci.* **2004**, *8*, 103–107. https://doi.org/10.5194/hess-8-103-2004.

52. Wischmeier, W.H.; Smith, D. *Predicting Rainfall Erosion Losses: A Guide to Conservation Planning (No. 537)*; *Department of Agriculture, Science and Education Administration: Washington, DC, USA*, 1978.

53. Panagos, P.; Meusburger, K.; Ballabio, C.; Borrelli, P.; Alewell, C. Soil erodibility in Europe: A high-resolution dataset based on LUCAS. *Sci. Total Environ.* **2014**, *479–480*, 189–200. https://doi.org/10.1016/j.scitotenv.2014.02.010.

54. Tóth, G.; Jones, A.; Montanarella, L. The LUCAS topsoil database and derived information on the regional variability of cropland topsoil properties in the European Union. *Environ. Monit. Assess.* **2013**, *185*, 7409–7425. https://doi.org/10.1007/s10661-013-3109-3.

55. Quinlan, J.R. Learning with continuous classes. In Proceedings of the Australian Joint Conference on Artificial Intelligence, Hobart, TAS, Australia, 16–18 November 1992; pp. 343–348.

56. Panagos, P.; Borrelli, P.; Poesen, J.; Ballabio, C.; Lugato, E.; Meusburger, K.; Montanarella, L.; Alewell, C. The new assessment of soil loss by water erosion in Europe. *Environ. Sci. Policy* **2015**, *54*, 438–447. https://doi.org/10.1016/j.envsci.2015.08.012.

57. Panagos, P.; Borrelli, P.; Meusburger, K.; van der Zanden, E.H.; Poesen, J.; Alewell, C. Modelling the effect of support practices (P-factor) on the reduction of soil erosion by water at European scale. *Environ. Sci. Policy* **2015**, *51*, 23–34. https://doi.org/10.1016/j.envsci.2015.03.012.

58. Panagos, P.; Borrelli, P.; Meusburger, K. A New European Slope Length and Steepness Factor (LS-Factor) for Modeling Soil Erosion by Water. *Geosciences* **2015**, *5*, 117–126. https://doi.org/10.3390/geosciences5020117.

59. Desmet, P.J.J.; Govers, G. A GIS procedure for automatically calculating the USLE LS factor on topographically complex landscape units. *J. Soil Water Conserv.* **1996**, *51*, 427–433.

60. Mashimbye, Z.E.; de Clercq, W.P.; Van Niekerk, A. An evaluation of digital elevation models (DEMs) for delineating land components. *Geoderma* **2014**, *213*, 312–319. https://doi.org/10.1016/j.geoderma.2013.08.023.

61. Olaya, V.; Conrad, O. *Chapter 12 Geomorphometry in SAGA*; *In Geomorphometry Concepts, Software, Applications, Developments in Soil Science; Hengl, T., Reuter, H.I., Eds.; Elsevier: Amsterdam, The Neatherlands, 2009; pp. 293–308.* ; pp. 293–308.

62. Estrada-Carmona, N.; Harper, E.B.; DeClerck, F.; Fremier, A.K. Quantifying model uncertainty to improve watershed-level ecosystem service quantification: A global sensitivity analysis of the RUSLE. *Int. J. Biodivers. Sci. Ecosyst. Serv. Manag.* **2017**, *13*, 40–50. https://doi.org/10.1080/21513732.2016.1237383.

63. Nearing, M.A.; Jetten, V.; Baffaut, C.; Cerdan, O.; Couturier, A.; Hernandez, M.; Le Bissonnais, Y.; Nichols, M.H.; Nunes, J.P.; Renschler, C.S.; et al. Modeling response of soil erosion and runoff to changes in precipitation and cover. *CATENA* **2005**, *61*, 131–154. https://doi.org/10.1016/j.catena.2005.03.007.

64. Almagro, A.; Oliveira, P.T.S.; Nearing, M.A.; Hagemann, S. Projected climate change impacts in rainfall erosivity over Brazil. *Sci. Rep.* **2017**, *7*, 8130. https://doi.org/10.1038/s41598-017-08298-y.

65. Buttafuoco, G.; Conforti, M.; Aucelli, P.P.C.; Robustelli, G.; Scarciglia, F. Assessing spatial uncertainty in mapping soil erodibility factor using geostatistical stochastic simulation. *Environ. Earth Sci.* **2012**, *66*, 1111–1125. https://doi.org/10.1007/s12665-011-1317-0.

66. Van der Knijff, J.M.F.; Jones, R.J.A.; Montanarella, L. *Soil Erosion Risk Assessment in Italy*; Office for Official Publications of the European Communities: Luxembourg, 1999.

67. Durigon, V.L.; Carvalho, D.F.; Antunes, M.A.H.; Oliveira, P.T.S.; Fernandes, M.M. NDVI time series for monitoring RUSLE cover management factor in a tropical watershed. *Int. J. Remote Sens.* **2014**, *35*, 441–453. https://doi.org/10.1080/01431161.2013.871081.

68. Pechanec, V.; Mráz, A.; Benc, A.; Cudlín, P. Analysis of spatiotemporal variability of C-factor derived from remote sensing data. *J. Appl. Remote Sens.* **2018**, *12*, 016022. https://doi.org/10.1117/1.JRS.12.016022.

69. Vatandaşlar, C.; Yavuz, M. Modeling cover management factor of RUSLE using very high-resolution satellite imagery in a semiarid watershed. *Environ. Earth Sci.* **2017**, *76*, 65. https://doi.org/10.1007/s12665-017-6388-0.

70. Vijith, H.; Seling, L.W.; Dodge-Wan, D. Effect of cover management factor in quantification of soil loss: Case study of Sungai Akah subwatershed, Baram River basin Sarawak, Malaysia. *Geocarto Int.* **2018**, *33*, 505–521. https://doi.org/10.1080/10106049.2016.1273398.

71. Main-Knorn, M.; Pflug, B.; Louis, J.; Debaecker, V.; Müller-Wilm, U.; Gascon, F. Sen2Cor for Sentinel-2. In Proceedings SPIE 10427, Image and Signal Processing for Remote Sensing XXIII; SPIE: 2017: Warsaw, Poland, 2017; Bruzzone, L., Bovolo, F., Benediktsson, J.A., Eds.; p. 3.

72. Hadjimitsis, D.G.; Papadavid, G.; Agapiou, A.; Themistocleous, K.; Hadjimitsis, M.G.; Retalis, A.; Michaelides, S.; Chrysoulakis, N.; Toulios, L.; Clayton, C.R.I. Atmospheric correction for satellite remotely sensed data intended for agricultural applications: Impact on vegetation indices. *Nat. Hazards Earth Syst. Sci.* **2010**, *10*, 89–95. https://doi.org/10.5194/nhess-10-89-2010.

73. Sola, I.; Alvarez-Mozos, J.; Gonzalez-Audicana, M. Inter-Comparison of Atmospheric Correction Methods on Sentinel-2 Images Applied to Croplands. In Proceedings of the IGARSS 2018—2018 IEEE International Geoscience and Remote Sensing Symposium, Valencia, Spain, 22–27 July 2018; IEEE publishing: 05 November 2018; pp. 5940–5943.

74. Alexakis, D.D.; Manoudakis, S.; Agapiou, A.; Polykretis, C. Towards the Assessment of Soil-Erosion-Related C-Factor on European Scale Using Google Earth Engine and Sentinel-2 Images. *Remote Sens.* **2021**, *13*, 5019. https://doi.org/10.3390/rs13245019.

75. Gallego, J.; Bamps, C. Using CORINE land cover and the point survey LUCAS for area estimation. *Int. J. Appl. Earth Obs. Geoinf.* **2008**, *10*, 467–475. https://doi.org/10.1016/j.jag.2007.11.001.

76. D'Andrimont, R.; Yordanov, M.; Martinez-Sanchez, L.; Eiselt, B.; Palmieri, A.; Dominici, P.; Gallego, J.; Reuter, H.I.; Joebges, C.; Lemoine, G.; et al. Harmonised LUCAS in-situ land cover and use database for field surveys from 2006 to 2018 in the European Union. *Sci. Data* **2020**, *7*, 352. https://doi.org/10.1038/s41597-020-00675-z.

77. Buchhorn, M.; Smets, B.; Bertels, L.; De Roo, B.; Lesiv, M.; Tsendbazar, N.E.; Herold, M.F. Copernicus Global Land Service: Land Cover 100m: Collection 3: Epoch 2015: Globe (Version V3.0.1). Available online: https://zenodo.org/record/3939038#.YZz08WDMK5c (accessed on 13 January 2022).

78. Buchhorn, M.; Smets, B.; Bertels, L.; De Roo, B.; Lesiv, M.; Tsendbazar, N.E.; Herold, M.F. Copernicus Global Land Service: Land Cover 100m: Collection 3: Epoch 2018: Globe (Version V3.0.1) Available online: https://zenodo.org/record/3518038#.YZz0V2DMK5c (accessed on 13 January 2022).

79. Gorelick, N.; Hancher, M.; Dixon, M.; Ilyushchenko, S.; Thau, D.; Moore, R. Google Earth Engine: Planetary-scale geospatial analysis for everyone. *Remote Sens. Environ.* **2017**, *202*, 18–27. https://doi.org/10.1016/j.rse.2017.06.031.

80. Borrelli, P.; Diodato, N.; Panagos, P. Rainfall erosivity in Italy: A national scale spatio-temporal assessment. *Int. J. Digit. Earth* **2016**, *9*, 835–850. https://doi.org/10.1080/17538947.2016.1148203.

81. Panagos, P.; Ballabio, C.; Borrelli, P.; Meusburger, K.; Klik, A.; Rousseva, S.; Tadić, M.P.; Michaelides, S.; Hrabalíková, M.; Olsen, P.; et al. Rainfall erosivity in Europe. *Sci. Total Environ.* **2015**, *511*, 801–814. https://doi.org/10.1016/j.scitotenv.2015.01.008.

82. Ayalew, D.A.; Deumlich, D.; Šarapatka, B. Agricultural landscape-scale C factor determination and erosion prediction for various crop rotations through a remote sensing and GIS approach. *Eur. J. Agron.* **2021**, *123*, 126203. https://doi.org/10.1016/j.eja.2020.126203.

83. Panagos, P.; Meusburger, K.; Van Liedekerke, M.; Alewell, C.; Hiederer, R.; Montanarella, L. Assessing soil erosion in Europe based on data collected through a European network. *Soil Sci. Plant. Nutr.* **2014**, *60*, 15–29. https://doi.org/10.1080/00380768.2013.835701.

84. Bircher, P.; Liniger, H.P.; Prasuhn, V. Comparing different multiple flow algorithms to calculate RUSLE factors of slope length (L) and slope steepness (S) in Switzerland. *Geomorphology* **2019**, *346*, 106850. https://doi.org/10.1016/j.geomorph.2019.106850.

85. Hickey, R. Slope Angle and Slope Length Solutions for GIS. *Cartography* **2000**, *29*, 1–8. https://doi.org/10.1080/00690805.2000.9714334.

86. Kienzle, S. The Effect of DEM Raster Resolution on First Order, Second Order and Compound Terrain Derivatives. *Trans. GIS* **2004**, *8*, 83–111. https://doi.org/10.1111/j.1467-9671.2004.00169.x.

87. Thompson, J.A.; Bell, J.C.; Butler, C.A. Digital elevation model resolution: Effects on terrain attribute calculation and quantitative soil-landscape modeling. *Geoderma* **2001**, *100*, 67–89. https://doi.org/10.1016/S0016-7061(00)00081-1.

88. Ayalew, D.A.; Deumlich, D.; Šarapatka, B.; Doktor, D. Quantifying the Sensitivity of NDVI-Based C Factor Estimation and Potential Soil Erosion Prediction using Spaceborne Earth Observation Data. *Remote Sens.* **2020**, *12*, 1136. https://doi.org/10.3390/rs12071136.

89. Borrelli, P.; Robinson, D.A.; Panagos, P.; Lugato, E.; Yang, J.E.; Alewell, C.; Wuepper, D.; Montanarella, L.; Ballabio, C. Land use and climate change impacts on global soil erosion by water (2015–2070). *Proc. Natl. Acad. Sci. USA* **2020**, *117*, 21994–22001. https://doi.org/10.1073/pnas.2001403117.

90. Märker, M.; Angeli, L.; Bottai, L.; Costantini, R.; Ferrari, R.; Innocenti, L.; Siciliano, G. Assessment of land degradation suscep-tibility by scenario analysis: A case study in Southern Tuscany, Italy. *Geomorphology* **2008**, *93*, 120–129. https://doi.org/10.1016/j.geomorph.2006.12.020.

91. Bargiel, D.; Herrmann, S.; Jadczyszyn, J. Using high-resolution radar images to determine vegetation cover for soil erosion assessments. *J. Environ. Manage.* **2013**, *124*, 82–90. https://doi.org/10.1016/j.jenvman.2013.03.049.

92. Almagro, A.; Thomé, T.C.; Colman, C.B.; Pereira, R.B.; Marcato Junior, J.; Rodrigues, D.B.B.; Oliveira, P.T.S. Improving cover and management factor (C-factor) estimation using remote sensing approaches for tropical regions. *Int. Soil Water Conserv. Res.* **2019**, *7*, 325–334. https://doi.org/10.1016/j.iswcr.2019.08.005.

93. Lunetta, R.S.; Knight, J.F.; Ediriwickrema, J.; Lyon, J.G.; Worthy, L.D. Land-cover change detection using multi-temporal MODIS NDVI data. *Remote Sens. Environ.* **2006**, *105*, 142–154. https://doi.org/10.1016/j.rse.2006.06.018.

94. Borrelli, P.; Meusburger, K.; Ballabio, C.; Panagos, P.; Alewell, C. Object-oriented soil erosion modelling: A possible paradigm shift from potential to actual risk assessments in agricultural environments. *L Degrad. Dev.* **2018**, *29*, 1270–1281. https://doi.org/10.1002/ldr.2898.

95. Yan, H.; Wang, L.; Wang, T.W.; Wang, Z.; Shi, Z.H. A synthesized approach for estimating the C-factor of RUSLE for a mixed-landscape watershed: A case study in the Gongshui watershed, southern China. *Agric. Ecosyst. Environ.* **2020**, *301*, 107009. https://doi.org/10.1016/j.agee.2020.107009.

96. Lal, R.; Reicosky, D.C.; Hanson, J.D. Evolution of the plow over 10,000 years and the rationale for no-till farming. *Soil Tillage Res.* **2007**, *93*, 1–12. https://doi.org/10.1016/j.still.2006.11.004.

97. Ruisi, P.; Giambalvo, D.; Saia, S.; Di Miceli, G.; Frenda, A.S.; Plaia, A.; Amato, G. Conservation tillage in a semiarid Mediterra-nean environment: Results of 20 years of research. *Ital. J. Agron.* **2014**, *9*, 1–7. https://doi.org/10.4081/ija.2014.560.

98. Veihe, A.; Hasholt, B.; Schiøtz, I.G. Soil erosion in Denmark: Processes and politics. *Environ. Sci. Policy* **2003**, *6*, 37–50. https://doi.org/10.1016/S1462-9011(02)00123-5.

99. Borrelli, P.; Robinson, D.A.; Fleischer, L.R.; Lugato, E.; Ballabio, C.; Alewell, C.; Meusburger, K.; Modugno, S.; Schütt, B.; Ferro, V.; et al. An assessment of the global impact of 21st century land use change on soil erosion. *Nat. Commun.* **2017**, *8*, 2013. https://doi.org/10.1038/s41467-017-02142-7.

100. Borrelli, P.; Paustian, K.; Panagos, P.; Jones, A.; Schütt, B.; Lugato, E. Effect of Good Agricultural and Environmental Conditions on erosion and soil organic carbon balance: A national case study. *Land Use Policy* **2016**, *50*, 408–421. https://doi.org/10.1016/j.landusepol.2015.09.033.

101. Panagos, P.; Ballabio, C.; Himics, M.; Scarpa, S.; Matthews, F.; Bogonos, M.; Poesen, J.; Borrelli, P. Projections of soil loss by water erosion in Europe by 2050. *Environ. Sci. Policy* **2021**, *124*, 380–392. https://doi.org/10.1016/j.envsci.2021.07.012.